Schottky peaks in specific heat induced by electronic change in the antiferromagnetic-ferromagnetic alternating Kondo systems Ce(Pd$_{1-x}$M$_x$)$_2$Al$_3$ (M=Cu or Ag)

Peijie Sun,[1] Qingfeng Lu,[2] Kentaro Kobayashi,[1] Tomohiko Kuwai,[1] and Yosikazu Isikawa[1]

[1]*Department of Physics, Toyama University, Toyama 930-8555, Japan*
[2]*Department of Physics, Henan Normal University, Henan 453002, People's Republic of China*

Kondo systems Ce(Pd$_{1-x}$M$_x$)$_2$Al$_3$ (M=Cu or Ag) have been previously shown to display antiferromagnetic (AFM) or ferromagnetic (FM) ordering alternatively then produce a complex phase diagram of AFM-FM-AFM type depending on the substitution amount x. This paper reports the results of specific heat $C(T)$ until high temperatures ($T \leq 150$ K) for the above systems. A Schottky peak is observed for all the samples in the magnetic contributions to specific heat, $C_{mag}(T)$, while deviating from a typical one on substitution. Unusual Schottky peaks that spread over a very wide temperature range with considerably small values can be confirmed at least around $x=0.2-0.3$ where FM ordering just occurs. The unusual Schottky peaks are phenomenologically associated with randomness in the crystal electric field induced by the Pd-M replacements, and the randomness is discussed as a probable origin of the AFM-FM transition. In addition, a comparison between the present systems and the relevant AFM-FM transition system CePd$_2$(Al$_{1-x}$Ga$_x$)$_3$ suggests that the mechanism for the FM ordering is different in the two cases.

PACS number(s): 75.30.Mb

I. INTRODUCTION

Investigations on rare-earth based ternary metallic compounds of the hexagonal PrNi$_2$Al$_3$-type have been of particular interest since the discovery of two well-known heavy fermion superconductors, UPd$_2$Al$_3$ and UNi$_2$Al$_3$, [1,2] focused on the diverse strongly correlated electronic effects including the Kondo effect, the Ruderman–Kittel–Kasuya–Yosida (RKKY) interaction and the crystal electric-field (CEF) splitting effect. In this crystal structure, Pr and Ni occupy the same basal planes that alternate with Al layers along the c axis. The discovery of CePd$_2$Al$_3$ (see Ref. 3), which shows antiferromagnetic (AFM) ordering at $T_N=2.8$ K and electronic specific-heat coefficient $\gamma \sim 380$ J/mol K^2, greatly supplements this family. Its magnetic structure has been determined by neutron diffraction measurements to be a type of ferromagnetic (FM) basal plane that is stacked antiferromagnetically along the c axis.[4]

So far, replacements of Pd atoms in CePd$_2$Al$_3$ with isoelectronic or nonisoelectronic transition metals while holding the crystal structure have shown diversely changed ground states. Among these, introducing isoelectronic atoms Ni yields a nonmagnetic ground state due to the volume effect on the hybridization between conduction and $4f$ electrons,[5,6] in good agreement with the hydrostatic pressure experiments.[7] While introducing nonisoelectronic atoms Cu (or Ag) gives rise to a complex phase diagram of AFM-FM-AFM type depending on the substitution amount x, and a decreasing tendency of Kondo temperature T_K.[8,9] Equally, substitutions with electronically different atoms drive magnetic-structure transitions in other systems as well, e.g., in CeNi$_{1-x}$Cu$_x$[10] and Ce(Pd$_{1-x}$Cu$_x$)$_2$Si$_2$.[11] This phenomenon is generally attributed to the electronic change therein induced, but the physical mechanisms in detail are diverse and still controversial.

On the other hand, surprisingly, a homologous compound CePd$_2$Ga$_3$ with Al replaced by isoelectronic Ga, was reported to exhibit FM ordering below $T_C \simeq 6$ K.[12,13] For CePd$_2$Ga$_3$, similarity to CePd$_2$Al$_3$ was found both in the CEF-derived energy scheme of Ce^{3+} and the magnetic anisotropy.[12,13] Based on comparative studies on the two compounds and their substitutional system CePd$_2$(Al$_{1-x}$Ga$_x$)$_3$,[14] the variation of the lattice parameter c with respect to a was suggested as the origin of the AFM-FM transition.[15] What supports this suggestion can be obtained from magnetic multilayers, where thickness-dependent oscillatory coupling (AFM or FM) between FM layers separated by a nonmagnetic metal spacer has been understood in the framework of the RKKY interaction,[16] considering the strong crystallographic resemblance between CePd$_2$(Al$_{1-x}$Ga$_x$)$_3$ and multilayers. Therefore, we believe the RKKY interaction serves as a basic interpretation on magnetic evolutions in rare-earth based compounds, with the exchange coupling oscillating with respect to the product $\kappa_F R$, where κ_F denotes the Fermi wave number and R the distance between magnetic ions in question.[17] The parameter R seems dominant in determining the magnetic structure of CePd$_2$(Al$_{1-x}$Ga$_x$)$_3$ as well as magnetic multilayers.

Situations in the present systems are apparently different from CePd$_2$(Al$_{1-x}$Ga$_x$)$_3$. This can be easily understood because of not only the electronic change in the present systems, but also the fact that closely similar phase diagrams were obtained for M=Cu and Ag in spite of their opposite evolutions on c/a. These evidences strongly imply that a second effect related to the electronic change might exist, dominating the magnetic evolution in Ce(Pd$_{1-x}$M$_x$)$_2$Al$_3$ (M=Cu or Ag).

Up to now, there are several descriptions apart from the oscillatory properties of the RKKY interaction attempting to interpret the magnetic-structure transition induced by elec-
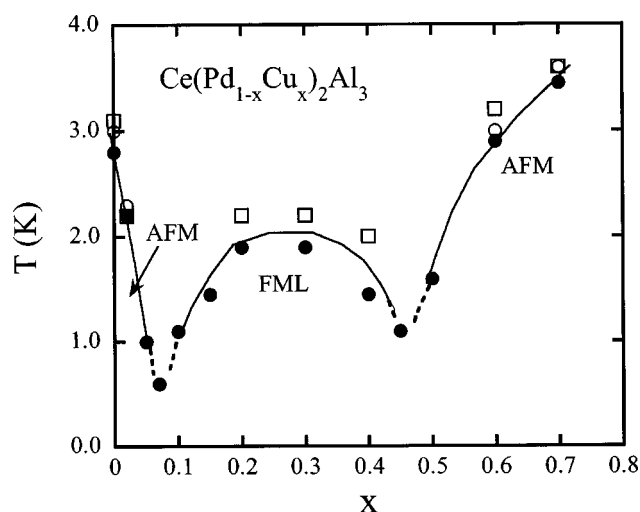
FIG. 1. Magnetic phase diagram of $Ce(Pd_{1-x}Cu_x)_2Al_3$. Closed circles, open circles and squares denote the magnetic transition temperatures determined by C, χ and ρ peaks, respectively (see Ref. 8).
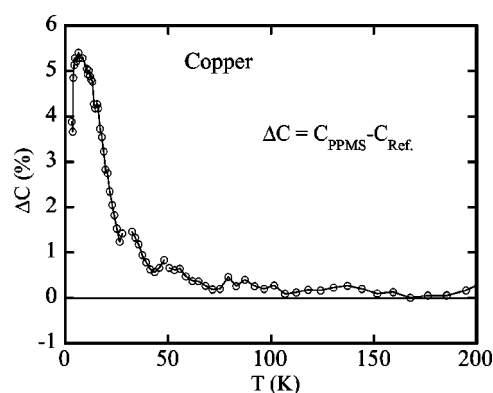

FIG. 2. Deviation in percentage of the present copper specific heat measured on the PPMS to that of the previous reports by Martin (see Ref. 22).

tronic change. For example, an extra FM interaction proportional to the density of states at the Fermi level is taken into account in addition to the proper RKKY interaction by Hernando et al.,[18] thus modification on the Fermi level may drive an AFM-FM transition. Studying the AFM-FM transition in $Tb_{1-x}Y_xNiAl$ and $TbNi_{1-x}Cu_xAl$, Ehlers et al. suggest a possible contribution from another indirect magnetic exchange coupling mechanism,[19] i.e., the one proposed by Campbell in the 1970's[20] and known to be parallel to the RKKY interaction to explain the magnetic ordering in rare earths. Additionally, Sereni, Beaurepaire, and Kappler speculate that the FM-AFM transition in $CePd_{1-x}Ag_x$ is due to the variation of the charge screening at the nonmagnetic sites.[21]

This paper is primarily stimulated by the observations of severe changes in magnetic anisotropy in the systems showing magnetic-structure transitions. Since the CEF effect is one of the effective factors in determining a magnetic structure and considerable information on it can be obtained from C_{mag} conveniently, we measured the specific heat until high temperatures for $Ce(Pd_{1-x}M_x)_2Al_3$ (M=Cu or Ag). To our surprise, the typical Schottky peak confirmed for x=0 is found unusual with replacements, especially around the intermediate concentrations of x where FM ordering emerges. This observation is discussed in the light of probable relationships among the unusual Schottky peaks, randomness in CEF and AFM-FM transitions.

The magnetic phase diagram of $Ce(Pd_{1-x}Cu_x)_2Al_3$ is extracted from our previous report[8] and is shown Fig. 1, where magnetic ordering temperature is plotted as a function of Cu concentration x. We can see immediately that an AFM region, then a ferromagnetic-like (FML) region, and at last a second AFM region emerges alternatively according to x. In fact, the FML state has been identified as ferromagnetic by well-defined hysteresis loop in magnetization experiments down to $T \sim 0.5$ K (not shown here). Similar phase diagram was obtained for the analogous $Ce(Pd_{1-x}Ag_x)_2Al_3$ system as well, on which a paper is in progress.[9] Entropy analysis proved that the ferromagnetism originates from the local mo-

ments of Ce^{3+} under CEF, the same as the antiferromagnetism. At high temperatures above 100 K, the effective magnetic moment μ_{eff} has a value of free Ce^{3+} with $J=5/2$ for the samples in the whole range of substitution.[8,9]

II. EXPERIMENTAL DETAILS

Polycrystalline samples $Ce(Pd_{1-x}M_x)_2Al_3$ (M=Cu or Ag) and selected La counterparts $La(Pd_{1-x}M_x)_2Al_3$ (x=0.0, 0.2, 0.4, and 0.6) were synthesized by arc melting the constituent elements and then annealing properly.[8,9] The well-defined single $PrNi_2Al_3$-type phase was found to extend to x=0.7 and to x=0.6 for M=Cu and Ag systems, respectively. The lattice parameters were determined by x-ray diffraction patterns on the powdered samples.

Specific heat measurements were performed by the relaxation technique, using a commercial physical properties measurement system (PPMS) (Quantum Design, Ltd.) with samples ranging from 20 to 50 mg. Samples were glued to the sample puck using Apiezon N grease to ensure good thermal contact, and the addenda (puck and grease) was measured just before each sample was studied. Part of the samples was measured down to $\sim$0.5 K with a quasiadiabatic method in an Oxford dilution refrigerator. C_{mag} was obtained by subtracting specific heat of a La counterpart as the lattice contribution from that of the corresponding Ce compound. For samples lacking a prepared La counterpart, the lattice contribution was estimated by scaling specific heat of other La compounds with x.

Prior to measurements on the samples, systematic errors in PPMS were analyzed by determining the specific heat of a copper sample (25.4 mg, purity 99.999%, without vacuum anneal) and comparing it with the well accepted values.[22] The results are shown in Fig. 2 for temperatures lower than 200 K, where the deviation appears as a plain curve without much scatter. The deviation is very small lower than 0.5% (typically 0.2% –0.3%) in the temperature range 60–300 K. Below 60 K, it grows rapidly with decreasing temperature, reaching 1% at $\sim$30 K and presenting a strange maximum over 5% around 7 K. Likewise, performance of PPMS on specific heat measurements has been examined by Lashley et

al.,[23] and our results resemble theirs strongly. The enhanced deviation at low temperatures was attributed to the difference in temperature scales and addenda errors by Lashley *et al.* and may partially come from the dissolved gas in pure copper sample.[24] Besides, one more uncertainty arises from mass measurements on a balance of 0.1 mg accuracy that we used. Attention was paid to minimize this uncertainty by averaging measurements up to ten times. Such a deviation in mass would lead to a regular and analyzable departure in specific heat, altering the C_{mag} peaks mainly on the height (e.g., within a magnitude of ± 0.3 J/mol K around 50 K), while leaving the width, which is emphasized in this paper, almost unchanged.

The abovementioned accuracy is tolerable for our discussion limited to $T \lesssim 150$ K considering the following matters: (1) the curve in Fig. 2 means an absolute deviation lower than 0.4 J/mol K (typically 0.2–0.3 J/mol K) for the samples in study over the temperature range $T \lesssim 150$ K, and the enhanced deviation at low temperatures does not drive large absolute deviation because of the small specific heat threat; (2) deviation of the same type is anticipated for both Ce and La compounds especially at low temperatures, in view of the regularity of the deviation derived by temperature scale, thus it may be partially cancelled in extracting C_{mag}; (3) little scatter is observed in the deviation curve; (4) reproducibilities were confirmed to be excellent by repeated measurements on our samples.

III. RESULTS AND ANALYSIS

In $Ce(Pd_{1-x}M_x)_2Al_3$, the evolution of the unit-cell volume with x is opposite for $M = Cu$ and Ag; Cu atoms reduce it and in contrast Ag atoms enlarge it. These trends are shown in Fig. 3(a). The ratio of the lattice parameters, c/a, which is a crucial parameter for the hexagonal structure, is also shown for the two cases in Fig. 3(b). Similar to the evolution of the unit-cell volume, c/a decreases when $M = Cu$ and increases when $M = Ag$.

Showing the lattice volume V and the c/a as a function of x is intended as a comparison not only between the present two systems of $M = Cu$ and Ag, but also between the present systems and the previously studied $CePd_2(Al_{1-x}Ga_x)_3$. In the latter case, c/a increases while V decreases with introducing Ga atoms into Al sites. This character in lattice is believed to be responsible for the magnetic-structure transition via the RKKY interaction.[15] Here, one should notice a substantial distinction between $Ce(Pd_{1-x}M_x)_2Al_3$ and $CePd_2(Al_{1-x}Ga_x)_3$, that is, the former changes the details in the Ce-contained basal planes while the latter modifies the Al layers.

In order to confirm the x-dependently systematic variation in total specific heat, in Fig. 4(a) we present the $C(T)$ curves for $Ce(Pd_{1-x}Cu_x)_2Al_3$ for several equal-interval concentrations ($x = 0.0$, 0.2, 0.4, and 0.6), along with two curves for $La(Pd_{1-x}Cu_x)_2Al_3$ ($x = 0.0$ and 0.6). It is for clarity that only part of our results are shown here. Apparently, magnetic contributions account for the majority of total specific heat below 10 K and a considerable part of it below about 30 K for all the Ce compounds. In higher temperatures close to 150 K, the change of $C(T)$ induced by substitution is very
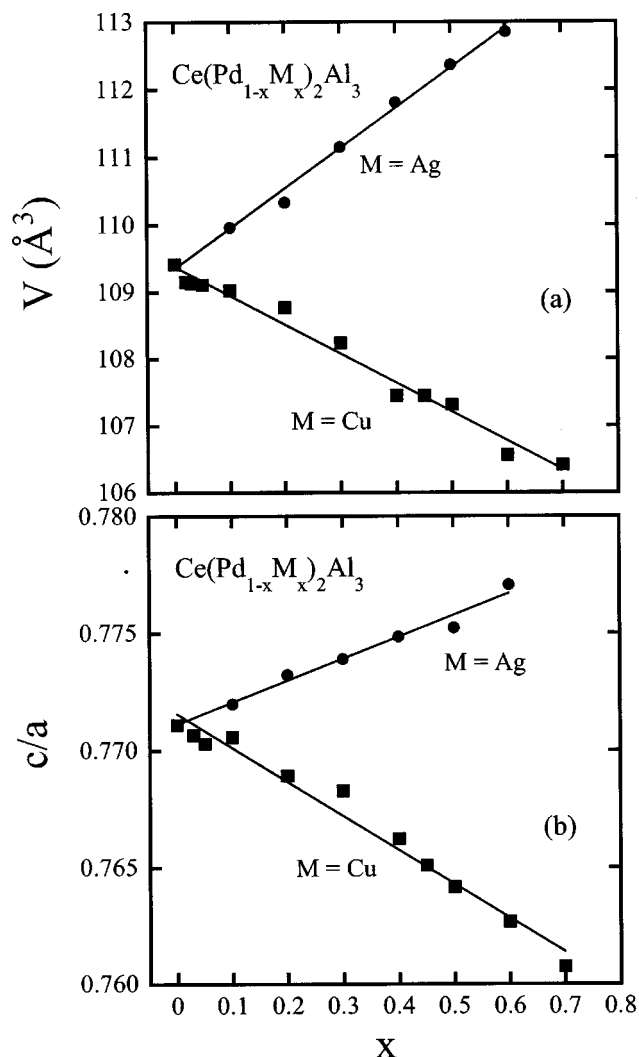

FIG. 3. Evolution of (a) the unit-cell volume and (b) the ratio of lattice parameters, c/a, as a function of substitution amount x for $Ce(Pd_{1-x}M_x)_2Al_3$ ($M = Cu$ or Ag). The lines serve as a guide for eyes.

weak. Nevertheless, systematic variation can be confirmed, as shown in the inset of Fig. 4(a), where C diminishes gradually with increasing x for both Ce and La compounds. Likewise, the system of $M = Ag$ shares the same descriptions given above.

Figure 4(b) displays the C/T vs T^2 curves for the low temperature range of $T < 8$ K for $La(Pd_{1-x}M_x)_2Al_3$. All the curves behave linearly according to the expression $C(T) = \gamma T + \beta T^3$, where γ represents electronic specific-heat coefficient and $\beta = 12\pi^4/5 \, Rv\theta_D^{-3}$ (R being the gas constant, v the number of atoms per formula unit and θ_D Debye temperature). Table I summarizes the γ and θ_D values obtained by least-squares fits for all the La compounds. Noteworthily, the Debye temperature θ_D increases with x when $M = Cu$ and decreases when $M = Ag$, reflecting the opposite changes in atom weights of Cu and Ag compared to Pd. On the other hand, γ decreases with x alike for both cases, indicative of a reduction of density of states at the Fermi level for conduction band. This is in accordance with the equivalent electronic structure of Cu and Ag atoms.
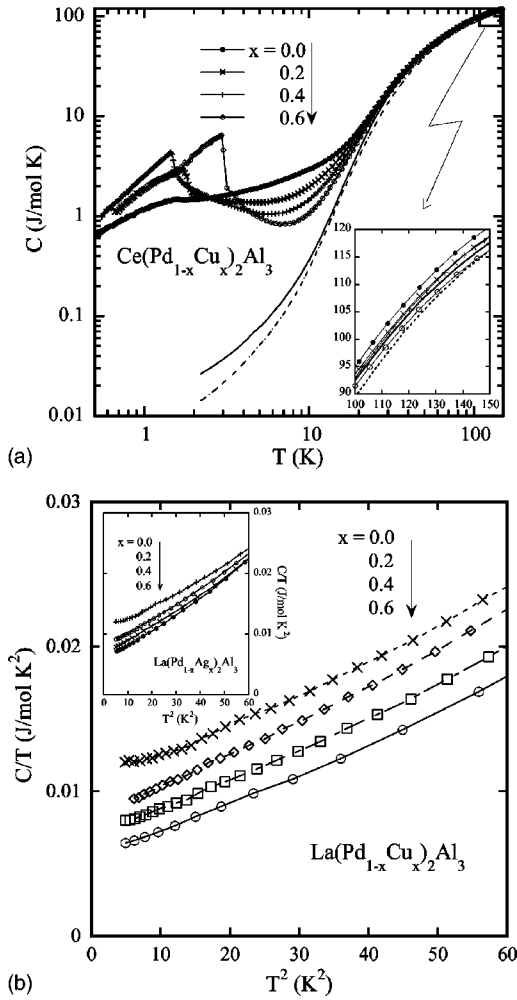
FIG. 4. (a) Total specific heat C as a function of temperature for several samples of Ce(Pd$_{1-x}$Cu$_x$)$_2$Al$_3$ with x=0.0, 0.2, 0.4, and 0.6. Both the horizontal and vertical axes are in a log scale. The solid and broken curves represent $C(T)$ of La(Pd$_{1-x}$Cu$_x$)$_2$Al$_3$ with x =0.0 and 0.6, respectively. The inset gives a close-up of the high temperature region in linear scales. (b) C/T vs T^2 curves for samples of La(Pd$_{1-x}$Cu$_x$)$_2$Al$_3$ with x=0.0, 0.2, 0.4, and 0.6, along with same curves for La(Pd$_{1-x}$Ag$_x$)$_2$Al$_3$ shown in the inset.

Figure 5 displays seven $C_{\text{mag}}(T)$ curves with equal x in-terval ($0 \leq x \leq 0.6$) for Ce(Pd$_{1-x}$Cu$_x$)$_2$Al$_3$. A close-up for the low temperature region of $T \leq 4$ K is attached to illustrate the evolution of the magnetic orderings, as has been shown as a phase diagram in Fig. 1.

The sixfold degenerate multiplet of Ce^{3+} splits into three doublets in the CEF potential of hexagonal symmetry, then producing Schottky peak in specific heat due to thermal ex-citations among different energy levels. This explains the peaks appearing at high temperatures in this system. Upon developing x, three outstanding features can be noticed within the tolerance of the specified uncertainties to charac-terize the evolution of the Schottky peak. First, the peak temperature grows up successively with increasing x till x =0.4, then saturates approximately to a certain value till x =0.6. Second, with increasing x the maximum value of the peak decreases initially in the range $0 \leq x \leq 0.2$, then in-

TABLE I. The electrical specific-heat coefficient γ and Debye temperature θ_D for La(Pd$_{1-x}$M$_x$)$_2$Al$_3$ (M=Cu or Ag) with x=0.0, 0.2, 0.4, and 0.6.

Compound	γ[mJ/mol K^2]	θ_D [K]
LaPd$_2$Al$_3$	9.7	369
La(Pd$_{0.8}$Cu$_{0.2}$)$_2$Al$_3$	8.1	373
La(Pd$_{0.6}$Cu$_{0.4}$)$_2$Al$_3$	6.9	389
La(Pd$_{0.4}$Cu$_{0.6}$)$_2$Al$_3$	5.4	394
La(Pd$_{0.8}$Ag$_{0.2}$)$_2$Al$_3$	7.7	364
La(Pd$_{0.6}$Ag$_{0.4}$)$_2$Al$_3$	6.5	362
La(Pd$_{0.4}$Ag$_{0.6}$)$_2$Al$_3$	5.6	357

creases till x=0.6. Third, in the intermediate x region includ-ing x=0.2 and 0.3, unusual Schottky peaks heavily broad-ened and deduced are exhibited. This behavior should be compared with the typical Schottky peak in x=0.0 and the relatively broadened but enhanced one in x=0.6.

The temperature T_{max} and the maximum value C_{max} of each Schottky peak were taken from Fig. 5, and are shown in Fig. 6 as a function of x. Shown in this figure are also those values for the equivalent system of M=Ag, whose specific heat would appear later in Fig. 8. Anomalous features in Fig. 6 are a valley in C_{mag} vs x curves and a relatively rapid growing of T_{max} around x=0.2–0.3.

Figure 7 highlights the $C_{\text{mag}}(T)$ curves for Ce(Pd$_{1-x}$Cu$_x$)$_2$Al$_3$ with x=0.0, 0.2, and 0.6 that each repre-sents a magnetically different region. Calculations based on the CEF-derived energy scheme of Ce^{3+} are performed to fit the data of x=0.0 and 0.6, but not the data of x=0.2. The reason is that for x=0.2, the large width and the lower values
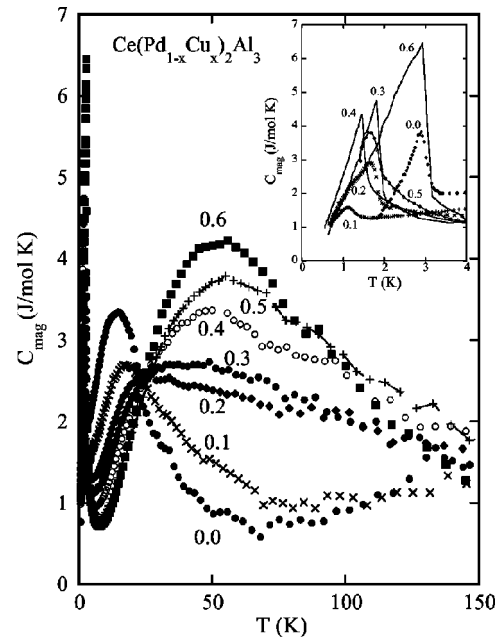

FIG. 5. Magnetic contribution to specific heat, C_{mag}, as a func-tion of temperature for Ce(Pd$_{1-x}$Cu$_x$)$_2$Al$_3$ with x=0.0, 0.1, 0.2, 0.3, 0.4, 0.5, and 0.6. The inset gives a close-up for low temperatures to illustrate the evolution of magnetic ordering.
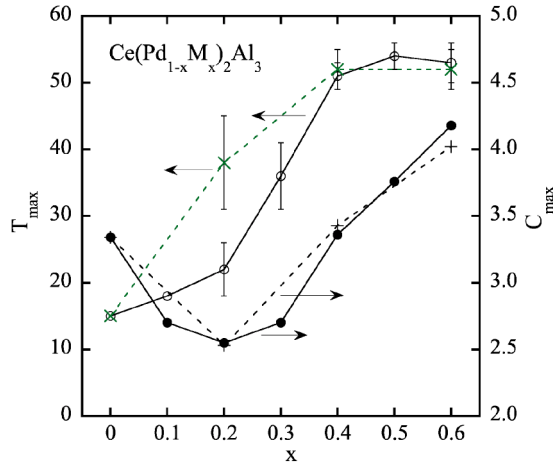
FIG. 6. The temperature, T_{max}, and the maximum value, C_{max}, of the Schottky peaks as a function of x for $M=Cu$ system (circles) and $M=Ag$ system (crosses) of $Ce(Pd_{1-x}M_x)_2Al_3$. The lines serve as a guide for eyes.

of the peak deviate itself far away from a typical Schottky type belonging to Ce^{3+}. The competition between the Kondo and CEF effects can reduce a Schottky peak but cannot broaden it so heavily.[25] Rather, it is not exaggerative to say that not a clear Schottky peak is established for $x=0.2$.

Fitting the data of $x=0.0$ we obtain $\triangle_1=33$ K and $\triangle_2 =500$ K, in agreement with the previously reported energy scheme that includes a ground doublet $\Gamma_7=|\pm1/2\rangle$ and two excited doublets $\Gamma_9=|\pm3/2\rangle$ at 33 K, $\Gamma_8=|\pm5/2\rangle$ over 600 K.[26] Somewhat higher peak in the fit curve can be explained by the moment reduction due to the Kondo effect of $T_K=19$ K in this compound. Discrepancy in $\triangle_2$ is tolerable in view of the differences in estimation procedures and systematic errors. For $x=0.6$, the peak grows up and seems perfect compared with that of $x=0.2$ and 0.3, however, the fit is rather tentative and qualitative still. Considering that the entropy achieved at 150 K exceeds the amount arising from a
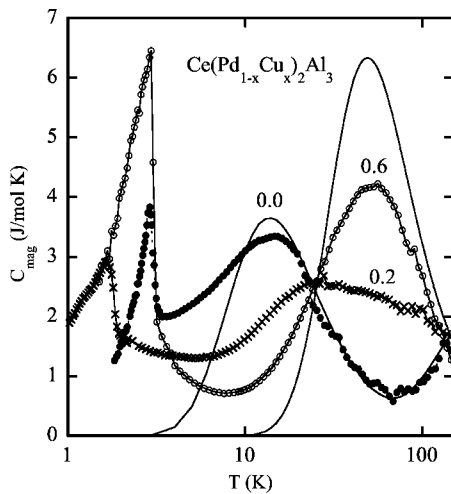

FIG. 7. Three selected $C_{mag}(T)$ curves for $Ce(Pd_{1-x}Cu_x)_2Al_3$ with $x=0.0$, 0.2, and 0.6. The lines represent theoretical calculations using the energy scheme $\triangle_1=33$ K, $\triangle_2=500$ K for $x=0.0$ and $\triangle_1 =\triangle_2=130$ K for $x=0.6$.
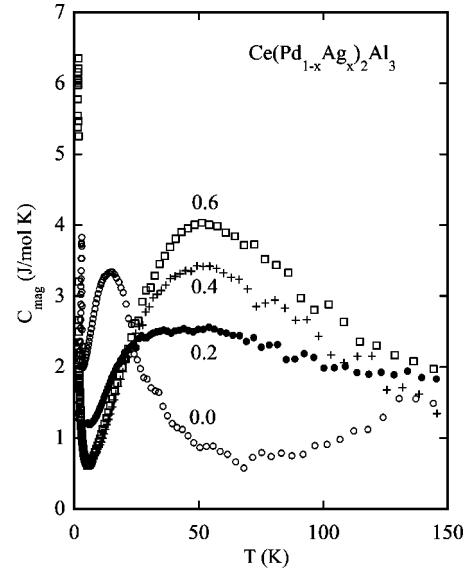

FIG. 8. Magnetic contribution to specific heat, C_{mag}, as a function of temperature for $Ce(Pd_{1-x}Ag_x)_2Al_3$ with $x=0.0$, 0.2, 0.4, and 0.6.

pair of doublets ($R \ln 4$) to a large degree (see Fig. 9), we propose an energy scheme with $\triangle_1 \simeq \triangle_2 \simeq 130$ K to fit the peak, which gives a reasonable position but much enhanced values. Apart from the Kondo effect, the same mechanism broadening and lowering the peak in $x=0.2$ should also be considered for $x=0.6$.

Figure 8 shows $C_{mag}(T)$ curves for $Ce(Pd_{1-x}Ag_x)_2Al_3$ for four typical samples with $x=0.0$, 0.2, and 0.6. These curves resemble their respective counterpart in $M=Cu$ system strikingly, with unusual Schottky peaks appearing in the intermediate region of x. Thus the two systems should share the same descriptions given above for Figs. 5–7.

Magnetic entropy curves $S_{mag}(T)$ are obtained by numerical integration of C_{mag}/T with respect to T and are shown in Fig. 9 for $Ce(Pd_{1-x}Cu_x)_2Al_3$. In Table II, the experimental
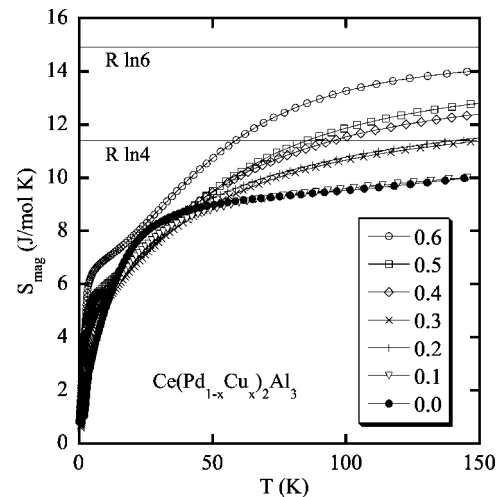

FIG. 9. Magnetic entropy S_{mag} derived from numerical integration of C_{mag}/T with respect to T, as a function of temperature for $Ce(Pd_{1-x}Cu_x)_2Al_3$.

TABLE II. The experimental minimum temperature, T_{ini}, the estimated initial value of entropy, S_{magL}, and the entropy amounted to at 150 K, S_{magH}, are tabulated for $Ce(Pd_{1-x}Cu_x)_2Al_3$.

x	T_{ini} (K)	S_{magL} (J/mol K)	S_{magH} (J/mol K)
0.0	1.82	1.1	10.0
0.1	0.67	1.1	10.1
0.2	0.66	1.0	11.5
0.3	0.64	0.6	11.4
0.4	0.55	0.8	12.4
0.5	1.42	2.8	12.8
0.6	1.44	2.4	14.0

minimum temperatures in our measurements, T_{ini}, the initial entropy at T_{ini} estimated by an extrapolation method, S_{magL}, and the entropy amounted to at 150 K, S_{magH}, are tabulated. Measurement errors may bring about considerable uncertainty to S_{magH} up to ± 1 J/mol K since it represents an integral number over a large temperature range, thus a precise analysis on $S_{\mathrm{mag}}(T)$ is not allowable. However, an increasing trend of S_{magH} with x is rather clear in the accuracy limit. For $x=0.0$ and 0.1, S_{mag} is lower considerably than $R \ln 4$ of the freedom from the lower-lying pair of doublets, then is enhanced by furthering x. For $x=0.6$, the S_{mag} is approaching $R \ln 6$ at 150 K, indicating that the six $4f$ states should be involved with the large Schottky peak. This inference is not contradictory with the fitting results shown in Fig. 7. Equally, enhancement of S_{magH} with x is also observed for the $M = Ag$ system.

IV. DISCUSSION AND SUMMARY

An important finding in our experimental results is the occurrence of unusual Schottky peaks, particularly around $x=0.2-0.3$ in $Ce(Pd_{1-x}M_x)_2Al_3$ ($M = Cu$ or Ag). These anomalies cannot be understood in the light of the competition between the Kondo and CEF effects, with the T_K decreasing upon increasing x.[8] According to the point charge CEF model, the $J=5/2$ multiplet of Ce^{3+} is split into three Kramers doublets of pure eigenstate in a hexagonal point-symmetry potential. These are $|\pm 1/2\rangle$, $|\pm 3/2\rangle$ and $|\pm 5/2\rangle$, as has been seen in $CePd_2Al_3$. The three pure eigenstates should persist even in the process of substitution as long as the point symmetry holds on. Thus only one matter remains, that is the rearrangement of the three pure eigenstates in the new energy scheme. However, our experimental results deviate apparently from this description.

The very broad and lower Schottky peaks around $x =0.2-0.3$ suggest a probability of Cu/Ag-induced randomness to CEF. As known, Pd atom is hole-like and Cu (or Ag) atom electron-like in view of their respective electronic structures. In the replacements, Cu (or Ag) atoms occupy the Pd sites (2c) randomly. The $4d$ shells of Pd ions may accept the valence electrons of Ce or Al atoms, becoming electrically neutral and nonmagnetic in the compounds, while the $3d$ (or $4d$) shells of the Cu (or Ag) ions are already completely filled. Consequently, Pd and Cu (or Ag) ions are elec-
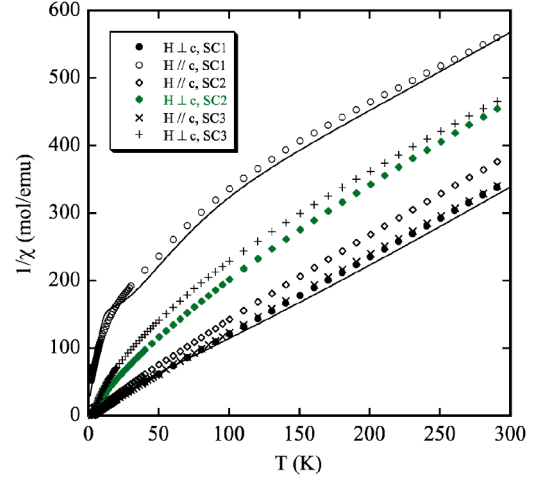

FIG. 10. Inverse magnetic susceptibility $\chi^{-1}(T)$ measured in an applied field 1 T for $CePd_2Al_3$ and 0.1 T for $Ce(Pd_{0.8}M_{0.2})_2Al_3$ ($M = Cu$ or Ag). The labels SC1, SC2, and SC3 denote the $CePd_2Al_3$, 20% Cu and 20% Ag substituted single crystals, respectively. The two solid lines are CEF calculations for $CePd_2Al_3$ with CEF parameters $B_2^0 = 18.6 K$, $B_4^0 = 0.24$ K and molecular-field constants $\lambda_{H\perp c} = \lambda_{H\parallel c} = 15$ mol/emu (Ref. 28).

trically different in the compounds. Taking this point into account, one can find immediately that unavoidable randomness in the distribution of Pd and Cu (or Ag) atoms would bring about randomness to CEF, even through the sample is macroscopically homogeneous. On the other hand, the Ce–Pd distance is even shorter than the Ce–Ce distance in $CePd_2Al_3$, thus the importance of the Ce–Pd ligand is furthermore anticipated in determining the Ce properties. We believe this randomness in CEF accounts for the unusual Schottky peaks in the present systems, and represents a common feature in substitutional systems of electronic change. For example, randomness in CEF was also noticed for $CeNi_{1-x}Cu_x$.[27]

Consistent evidence would be found in our recent magnetic susceptibility results on the single crystals including $CePd_2Al_3$ and $Ce(Pd_{0.8}M_{0.2})_2Al_3$ ($M = Cu$ or Ag), as shown in Fig. 10.[28] In comparison to $CePd_2Al_3$ that has in-plane magnetic moments, weakened and reversed magnetic anisotropy is found in the latter two FM compounds with easy direction of magnetization along the c axis. Fitting the data of $CePd_2Al_3$ by the point charge CEF model, we obtained a reasonable energy scheme of $\triangle_1 \simeq 40$ K and $\triangle_2 \simeq 320$ K, while fits to the FM compounds failed to give plausible results. Nevertheless, in the CEF model such a reverse of magnetic anisotropy means at least a change of the sign of the dominating CEF parameter B_2^0 and a replacement of the ground level $|\pm 1/2\rangle$. A consequent overturn between energy levels would cause a quartet ground state at a certain amount of substitution, however, it was not detected by our experiments including specific heat. Therefore, the abovementioned facts support the inference of Cu/Ag-induced randomness in CEF, in which the notion of three pure eigenstates collapses.

The importance of CEF in determining magnetic structure is demonstrated here by giving $PrNi_{5-x}Cu_x$, in which both

$PrNi_5$ and $PrCu_5$ are nonmagnetic with a CEF-derived singlet ground state.[29] Surprisingly, FM ordering was observed in $PrNi_{5-x}Cu_x$ for $0.9 \leqslant x \leqslant 2.6$, whose mechanism was at first attributed to the enhancement of $3d$ band susceptibility which in turn enhances the exchange interaction among Pr ions.[29] However, taking $PrNi_{3.9}Cu_{0.1}$ as an example, Liu *et al.* argue by theoretical calculations that the origin of the FM ordering results from a mixing of excited CEF levels with ground state.[30] This mixing arises from the distorted CEF induced by substituting Cu for Ni atoms. One difference between $PrNi_{5-x}Cu_x$ and $Ce(Pd_{1-x}M_x)_2Al_3$ is that Ni and Cu ions have respective preferable sites ($3g$ for Ni and $2c$ for Cu) in the former system while replacements are random in the latter, hence distortion and randomness happen to CEF for the two cases, respectively. The randomness in CEF prevents one from estimating the specific eigenstates for the present systems. However, associating the facts that the in-plane exchange coupling is FM at low temperatures showing strong anisotropy for $CePd_2Al_3$, we speculate that the change in CEF may break the unique AFM structure and may lead to the AFM-FM transition.

Questions then arise, whether we can say samples with higher x (such as, $x=0.6$) are diminishing the randomness in CEF because they are shifting their Schottky peaks to a typical one of point charge CEF, and why do they not order ferromagnetically like the intermediate region. Clarifying these queries is very difficult at the moment, while two points of view are definite and useful in the understanding of them. First, although analysis on Schottky peak is a convenient method to investigate CEF with an energy scheme, it provides no information on the knowledge of state functions. Thus, other investigations, preferably on single crystals, are necessary to study the randomness in CEF for higher x region. Second, the exchange interaction of the RKKY type would be changed gradually by introducing Cu (or Ag) atoms to Pd sites and modifying κ_F. This is known as a normal

evolution of the RKKY interaction, and is able to drive a magnetic-structure transition. So, it is insufficient to take only the randomness in CEF into account for the higher x region.

It is of particular interest to make a comparison between $Ce(Pd_{1-x}M_x)_2Al_3$ ($M=$Cu or Ag) and $CePd_2(Al_{1-x}Ga_x)_3$ with respect to the substitutional effects on the magnetic structures. Elastic neutron scattering experiments show that the ground state keeps unchanged in the latter system when Al atoms are replaced by iso-electronic Ga atoms.[12,13,26] Furthermore, the energy scheme and the magnetic anisotropy are also very alike for both the Al and Ga ends. All these parallel properties in $CePd_2(Al_{1-x}Ga_x)_3$ are easy to be concerned with the iso-electronic structures of Al and Ga atoms. Consequently, it is reasonable to propose that the difference in atomic radius serves as an intrinsic origin in the magnetic-structure transition in $CePd_2(Al_{1-x}Ga_x)_3$, by changing c/a.[15] This description is acceptable in the framework of the RKKY interaction. However, in $Ce(Pd_{1-x}M_x)_2Al_3$ ($M=$Cu or Ag), it is not the lattice variation but the electronic change that dominates the magnetic evolution.

To summarize, we observed identical evolutions of Schottky peaks in the Kondo systems $Ce(Pd_{1-x}M_x)_2Al_3$ with M being Cu and Ag atoms. Unusual Schottky peaks that are much lower and broad were found around $x=0.2-0.3$, which reminds us of the occurrence of FM orderings in this region, thus their relationship is discussed. The randomness in CEF potential, which originates from the random distribution of Cu (or Ag) atoms, is speculated to drive the unusual Schottky peaks, and lead to the AFM-FM transition. A comparison between the present systems and $CePd_2(Al_{1-x}Ga_x)_3$ suggests different mechanisms for the magnetic-structure transitions in the two cases. Theoretical analyses in terms of CEF on the magnetic phase diagrams of the present systems are greatly desirable.

[1] C. Geibel, S. Thies, D. Kaczorowski, A. Mehner, A. Grauel, B. Seidel, U. Ahlheim, R. Helfrich, K. Petersen, C. D. Bredl, and F. Steglich, Z. Phys. B: Condens. Matter **83**, 305 (1991).

[2] C. Geibel, C. Schank, S. Thies, H. Kitazawa, C. D. Bredl, A. Böhm, M. Rau, A. Grauel, R. Caspary, R. Helfrich, U. Ahlheim, G. Weber, and F. Steglich, Z. Phys. B: Condens. Matter **84**, 1 (1991).

[3] H. Kitazawa, C. Schank, S. Thies, B. Seidel, C. Geibel, and F. Steglich, J. Phys. Soc. Jpn. **61**, 1461 (1992).

[4] S. Mitsuda, T. Wada, K. Hosoya, H. Yoshizawa, and H. Kitazawa, J. Phys. Soc. Jpn. **61**, 4667 (1992).

[5] Y. Isikawa, H. Sakai, T. Mizushima, T. Kuwai, and J. Sakurai, Physica B **312,313**, 259 (2002).

[6] E. Bauer, A. Galatanu, P. Rogl, M. Gómez Berisso, P. Pedrazzini, and J. G. Sereni, Physica B **312,313**, 464 (2002).

[7] F. Nolting, A. Eichler, S. A. M. Mentink, and J. A. Mydosh, Physica B **199,200**, 614 (1994).

[8] P. Sun, Y. Isikawa, Q. Lu, D. Huo, and T. Kuwai, J. Phys. Soc. Jpn. **72**, 916 (2003).

[9] P. Sun *et al.* (unpublished).

[10] J. García Soldevilla, J. C. Gómez Sal, J. A. Blanco, J. I. Espeso, and J. Rodríguez Fernández, Phys. Rev. B **61**, 6821 (2000).

[11] M. Gomez Berisso, O. Trovarelli, P. Pedrazzini, G. Zwicknagl, C. Geibel, F. Steglich, and J. G. Sereni, Phys. Rev. B **58**, 314 (1998).

[12] E. Bauer, R. Hauser, E. Gratz, G. Schaudy, M. Rotter, A. Lindbaum, D. Gignoux, and D. Schmitt, Z. Phys. B: Condens. Matter **92**, 411 (1993).

[13] E. Bauer, G. Schaudy, G. Hilscher, L. Keller, P. Fischer, and A. Dönni, Z. Phys. B: Condens. Matter **94**, 359 (1994).

[14] B. Ludoph, S. Süllow, B. Becker, G. J. Nieuwenhuys, A. A. Menovsky, and J. A. Mydosh, Physica B **223,224**, 351 (1996).

[15] T. Burghardt, E. Hallmann, and A. Eichler, Physica B **230–232**, 214 (1997); T. Burghardt, A. Eichler, S. Süllow, and J. A. Mydosh, *ibid.* **259–261**, 99 (1999).

[16] P. Bruno and C. Chappert, Phys. Rev. Lett. **67**, 1602 (1991).

[17] K. Yosida, Phys. Rev. **106**, 893 (1957).

[18] A. Hernando, J. M. Rojo, J. C. Gómez Sal, and J. M. Novo, J.

Appl. Phys. **79**, 4815 (1996); A. Hernando, J. M. Barandiarán, J. M. Rojo, and J. C. Gómez Sal, J. Magn. Magn. Mater. **174**, 181 (1997).

[19] G. Ehlers, C. Ritter, A. Krutjakow, W. Miekeley, N. Stüßer, Th. Zeiske, and H. Maletta, Phys. Rev. B **59**, 8821 (1999).

[20] I. A. Campbell, J. Phys. F: Met. Phys. **2**, L47 (1972).

[21] J. G. Sereni, E. Beaurepaire, and J. P. Kappler, Phys. Rev. B **48**, 3747 (1993).

[22] D. L. Martin, Phys. Rev. **141**, 576 (1966); D. L. Martin, Rev. Sci. Instrum. **58**, 639 (1987).

[23] J. C. Lashley, M. F. Hundley, A. Migliori, J. L. Sarrao, P. G. Pagliuso, T. W. Darling, M. Jaime, J. C. Cooley, W. L. Hults, L. Morales, D. J. Thoma, J. L. Smith, J. Boerio-Goates, B. F. Woodfield, G. R. Steward, R. A. Fisher, and N. E. Phillips, Cryogenics **43**, 369 (2003).

[24] D. L. Martin, Rev. Sci. Instrum. **38**, 1738 (1967).

[25] See, for example, Y. Shimizu and O. Sakai, J. Phys. Soc. Jpn. **65**, 2632 (1996), where theoretical calculations on specific heat are carried out considering both the Kondo effect and CEF interaction.

[26] S. A. M. Mentink, G. J. Nieuwenhuys, A. A. Menovsky, J. A. Mydosh, H. Tou, and Y. Kitaoka, Phys. Rev. B **49**, 15 759 (1994).

[27] J. C. Gómez Sal, J. I. Espeso, J. García Soldevilla, J. Rodríguez Fernández, and J. A. Blanco, Physica B **281,282**, 42 (2000).

[28] P. Sun, Y. Isikawa, K. Kobayashi, T. Mizushima, and T. Kuwai, in *Proceedings of the International Conference on Strongly Correlated Electron Systems* (Karlsruhe, Germany 2004).

[29] A. G. Kuchin, A. S. Ermolenko, V. I. Khrabrov, G. M. Makarova, and E. V. Belozerov, J. Magn. Magn. Mater. **159**, L309 (1996).

[30] Z.-S. Liu and J.-G. Park, Physica B **322**, 133 (2002).